# Unequivocal Identification of Spin-Triplet and Spin-Singlet Superconductors with Upper Critical Field and Flux Quantization

C. C. Chiang,[1,2] H. C. Lee,[1] S. C. Lin,[3] D. Qu,[3,4] M. W. Chu,[3,4] C. D. Chen,[5] C. L. Chien,[1,2,*] and S. Y. Huang[1,4,†]

[1]*Department of Physics, National Taiwan University, Taipei 10617, Taiwan*

[2]*Willian H. Miller III Department of Physics and Astronomy, Johns Hopkins University, Baltimore, Maryland 21218, USA*

[3]*Center for Condensed Matter Sciences, National Taiwan University, Taipei 10617, Taiwan*

[4]*Center of Atomic Initiatives for New Materials, National Taiwan University, Taipei 10617, Taiwan*

[5]*Institute of Physics, Academia Sinica, Taipei 11529, Taiwan*

(Received 4 August 2023; accepted 13 November 2023; published 5 December 2023)

Spin-triplet superconductors play central roles in Majorana physics and quantum computing but are difficult to identify. We show the methods of kink-point upper critical field and flux quantization in superconducting rings can unequivocally identify spin-singlet, spin-triplet in centrosymmetric superconductors, and singlet-triplet admixture in noncentrosymmetric superconductors, as realized in $\gamma$-BiPd, $\beta$-$Bi_2Pd$, and $\alpha$-BiPd, respectively. Our findings are essential for identifying triplet superconductors and exploring their quantum properties.

DOI: 10.1103/PhysRevLett.131.236003

Exploring quantum materials for quantum computation has attracted much attention in recent years. Notably, superconducting qubits have emerged as the leading contender for a scalable quantum computing platform, achieving quantum supremacy with 53 superconducting qubits in 2019 [1]. Notwithstanding the impressive advances, theories indicate topological triplet superconductors (SCs) play central roles in Majorana fermions physics and fault-tolerant quantum computing [2–4]. Indeed, the search for topological triplet SCs has been a long-standing research focus in condensed matter physics, where unequivocal identification of singlet and triplet SCs is of paramount importance.

Bose-Einstein condensation of Cooper pairs below the transition temperature $T_C$ gives rise to superconductivity. The Cooper pairs can be either spin singlet with spin 0 ($s$ wave and $d$ wave) with even parity or spin-triplet with spin 1 ($p$-wave) with odd parity. To date, the known SCs are overwhelmingly singlet, mostly $s$ wave (e.g., Nb) and some $d$ wave (e.g., cuprates). Triplet SCs with $p$-wave pairing, important for Majorana physics, quantum computing, and spin supercurrent, are very rare. The most well-known $p$-wave prospect may be $Sr_2RuO_4$ for over 20 yr [5]. However, the compelling Knight shift results for $p$-wave pairing have recently been overturned, thus ending its spin-triplet prospect [6,7]. These events highlight the importance of reliable assessment of singlet and triplet SCs. In the past, measurements of thermodynamic properties, such as penetration depth, upper critical field, and specific heat, have been used but unable to decisively identify triplet pairing in SCs.

The phase-sensitive method for detecting the sign change of the superconducting gap has been instrumental for assessing SCs since revealing the $d$-wave pairing in cuprates via tricrystals and corner junctions [8,9]. The observation of half-integer flux of $(n + ½)\Phi_o$, where $\Phi_o = hc/2e$, $h$ is the Planck's constant, $c$ the speed of light, $e$ the electronic charge, and $n$ an integer in the flux quantization (Little-Parks effect) experiments in rings reveals the triplet pairing in $\beta$-$Bi_2Pd$ [10]. However, phase-sensitive methods require the fabrication of μm sized devices such as tricrystals, corner junctions, and rings. Recently, a new method of identifying triplet pairing by exploiting the kink point in the upper critical field $H_{c2}$ has been demonstrated in $UTe_2$ [11] and $CeRh_2As_2$ [12]. It is of great importance to apply the two methods of half-integer quantum flux and kink point in $H_{c2}$ to the *same* materials for rigorously assessing their abilities in identifying singlet and triplet SCs.

The parity symmetry of SCs plays a crucial role in determining the possible pairing states. For centrosymmetric SCs with inversion symmetry, as in most SCs, the pairing state must be either an even-parity spin-singlet state or an odd-parity spin-triplet state. However, for noncentrosymmetric SCs, the absence of inversion symmetry necessitates an admixture of singlet and triplet pairing states. The unusual BiPd in this work exists in two structures with different symmetries: centrosymmetric $\gamma$-BiPd and noncentrosymmetric $\alpha$-BiPd. Although the noncentrosymmetric $\alpha$-BiPd exhibits an interesting Dirac surface state from angle-resolved photoemission spectroscopy (ARPES), the topological surface states (TSSs) in $\alpha$-BiPd are absent at the Fermi level ($E_F$) and thus not topological SC [13,14]. However, because of the noncentrosymmetric nature, $\alpha$-BiPd is an admixture of singlet-triplet pairing. On the other hand, the centrosymmetric

 

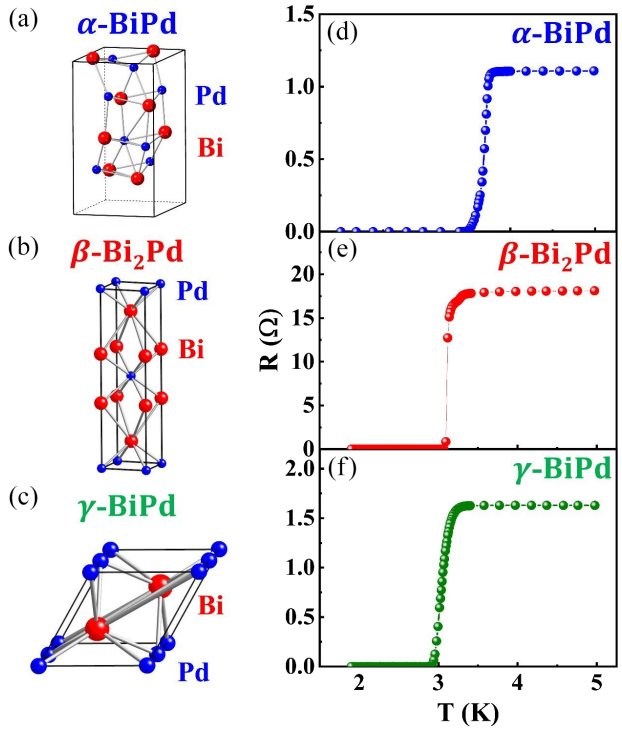


FIG. 1. The crystal structure of (a) $\alpha$-BiPd, (b) $\beta$-$Bi_2Pd$, and (c) $\gamma$-BiPd. The temperature dependence of the resistance of the superconductors of (d) $\alpha$-BiPd, (e) $\beta$-$Bi_2Pd$, and (f) $\gamma$-BiPd.

$\beta$-$Bi_2Pd$ with the TSSs at $E_F$, hence a topological SC with the profound connection to spin-triplet pairing [15]. The SCs of $\gamma$-BiPd, $\beta$-$Bi_2Pd$, and $\alpha$-BiPd thus provide a unique test bed for distinguishing singlet, triplet, and admixture of singlet and triplet using the two methods of kink-point $H_{c2}$ and flux quantization.

We use magnetron co-sputtering from Bi and Pd sources to deposit 50 nm thin films of BiPd and $\beta$-$Bi_2Pd$ on thermally oxidized Si substrates. The relative deposition rates control the material composition, subsequently determined by an electron probe x-ray microanalyzer. Thin films of $\beta$-$Bi_2Pd$ and $\gamma$-BiPd are deposited at 400 and 200° C, respectively. Interestingly, after post-annealing at an elevated temperature of 270° C, the centrosymmetric $\gamma$-BiPd transforms into noncentrosymmetric $\alpha$-BiPd. We use x-ray reflectometry for measuring film thickness, atomic force microscopy for surface roughness, and x-ray diffraction for crystal structures and film orientations. For the flux quantization (Little-Parks effect) measurement, we pattern thin films into sub-μm ring devices with linewidths of about 100 nm by electron beam lithography.

As shown in Figs. 1(a)–1(c), the crystal structure of $\alpha$-BiPd is noncentrosymmetric with space group $P2_1$, and that of $\beta$-$Bi_2Pd$ and $\gamma$-BiPd are centrosymmetric with space group $I_4/mmm$ and $P6_3$ [16], respectively. X-ray diffraction with pole-figure measurements indicates that $\alpha$-BiPd films are $(1\bar{1}2)$ textured, $\beta$-$Bi_2Pd$ films are (001) textured, and $\gamma$-BiPd films are (011) textured, as shown in Figs. S1(a)–S1(c), respectively, without in-plane epitaxy (see Supplemental Material [17]). Importantly, the $\alpha$-BiPd, $\beta$-$Bi_2Pd$, and $\gamma$-BiPd films display superconductivity with $T_C$ of 3.7, 3.6, and 3.3 K, respectively, as evidenced by the sharp transitions shown in Figs. 1(d)–1(f).

We first explore the temperature sweep results of the upper critical field $H_{c2}$ by measuring temperature-dependent resistivity at various constant magnetic fields applied parallel and also perpendicular to the film planes. When the measurement temperatures are close to $T_C$ in the smaller magnetic field region, the transition from normal to superconducting states is very sharp in all the BiPd thin films, regardless of the field direction. Figures 2(c) and S3(c) show the results of $\gamma$-BiPd films under the out-of-plane and in-plane magnetic field, respectively, where the narrow transition width remains essentially unchanged. Since the thickness of the thin films restricts the perpendicular coherence length, there is an anisotropy of the upper critical field of $H_{c2\perp}(T) < H_{c2\parallel}(T)$, as described by the Ginzburg-Landau (GL) equation [19],

$$H_{c2\perp}(T) = \frac{\phi_0}{2\pi\xi_{\mathrm{GL}}^2(0)}\left(1-\frac{T}{T_c}\right), \tag{1}$$

and

$$H_{c2\parallel}(T) = \frac{\sqrt{12}\phi_0}{2\pi\xi_{\mathrm{GL}}(0)d_s}\sqrt{\left(1-\frac{T}{T_c}\right)}, \tag{2}$$

where $\phi_0$ is the flux quantum, $\xi_{GL}(0)$ is the 0 K value of GL coherence length, and $d_s$ is the thickness of SC. Figure 2(c) illustrates that the $H_{c2}$(T) behavior of $\gamma$-BiPd films can be accurately described by the GL formulas (and is also applicable to Nb thin films, as shown in the Supplemental Material [17]).

However, for $\alpha$-BiPd and $\beta$-$Bi_2Pd$ thin films, the transition width instead increases at higher magnetic fields and lower temperatures for out-of-plane [Figs. 2(a) and 2(b)] and in-plane [Fig. S3(a) and S3(b)] fields, respectively. The $H_{c2}$(T) behavior satisfies the GL relation only at temperatures higher than about 2.5 K before deviating at lower temperatures. The estimated $\xi_{\mathrm{GL}}(0)$ value for $\alpha$-BiPd, $\beta$-$Bi_2Pd$, and $\gamma$-BiPd are approximately 21, 15, and 15 nm, respectively. Consequently, $\alpha$-BiPd and $\beta$-$Bi_2Pd$ thin films show a distinct kink behavior in $H_{c2\perp}(T)$ and $H_{c2\parallel}(T)$, as shown in Figs. 2(d), 2(g), 2(e), and 2(h), similar to those observed in $UTe_2$ [11] and $CeRh_2As_2$ [12] that has been associated with triplet pairing.

In conventional SCs, the $H_{c2}$ is limited by the combined effects of orbital and paramagnetic pair breaking. For comparison, we estimate the 0 K orbital limit by the Werthamer-Helfand-Hohenberg theory $H_{\mathrm{orb}} \approx 0.693T_c(-(dH_{c2}/dT))_{T_c}$ [20,21] yielding $H_{\mathrm{orb}} = 2.47$,

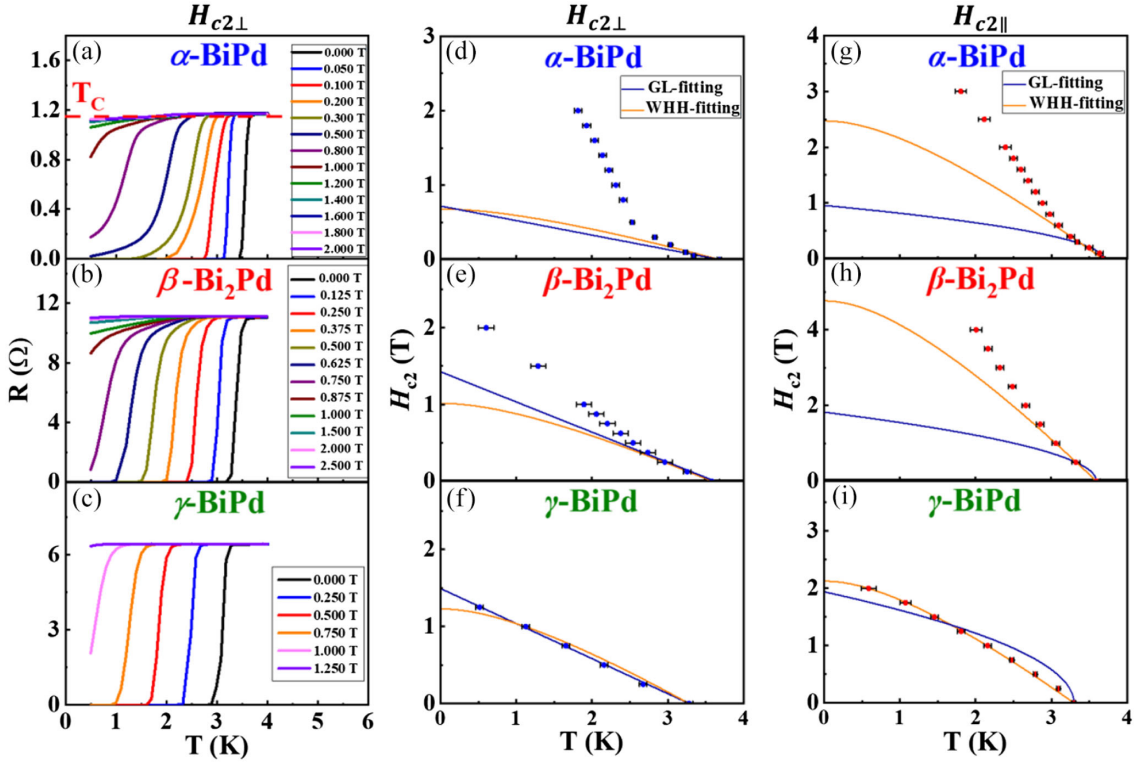


FIG. 2. The temperature sweep results of the upper critical field $H_{c2}$ by measuring temperature-dependent resistivity at various constant magnetic fields applied perpendicular to the film planes in (a) $\alpha$-BiPd, (b) $\beta$-$Bi_2Pd$, and (c) $\gamma$-BiPd. The temperature dependence of the upper critical field in (d) $\alpha$-BiPd, (e) $\beta$-$Bi_2Pd$, (f) $\gamma$-BiPd with the out-of-plane magnetic field, and (g) $\alpha$-BiPd, (h) $\beta$-$Bi_2Pd$, and (i) $\gamma$-BiPd with the in-plane field. The blue and orange solid curves are fitted by the GL relationships and WHH theory, respectively.

4.76, and 2.13 T for $\alpha$-BiPd, $\beta$-$Bi_2Pd$, and $\gamma$-BiPd, respectively (see [17] for the detailed calculation and fitting results). The Pauli limit of $H_{\mathrm{para}}(0) = 1.86T_c$, gives 6.88, 6.70, and 6.14 T for $\alpha$-BiPd, $\beta$-$Bi_2Pd$, and $\gamma$-BiPd, respectively. Unlike $UTe_2$ and $CeRh_2As_2$ with $H_{\mathrm{orb}} > H_{\mathrm{para}}$, all BiPd SCs show $H_{\mathrm{orb}} < H_{\mathrm{para}}$. As a result, the kink behavior of $\alpha$-BiPd and $\beta$-$Bi_2Pd$ exceeds the orbital pair-breaking limit, while $\gamma$-BiPd is strongly orbital limited. Our results suggest that field-induced unconventional transition is a vital feature of the spin-triplet state instead of a large critical field.

In contrast, the $H_{c2}(T)$ curve of $\gamma$-BiPd films displays no kink behavior and only a conventional BCS behavior, as shown in Figs. 2(f) and 2(i), whereas $H_{c2}$ of both $\alpha$-BiPd and $\beta$-$Bi_2Pd$ exhibits the highly unusual kink-point behavior. The kink points in $\alpha$-BiPd and $\beta$-$Bi_2Pd$ indicate the intrinsic pairing difference. As revealed by the second method—flux quantization measurement described below, $\beta$-$Bi_2Pd$ and $\alpha$-BiPd with half-quantization affirm the triplet pairing in SCs, whereas $\gamma$-BiPd with integer-quantization shows pure-singlet pairing. Therefore, by supporting the flux-quantization measurement, we demonstrate that the unusual kink-point indicates the triplet pairing in SC. The kink point in $H_{c2}$ can indeed identify triplet pairing.

We next present the field-sweep $H_{c2}$ results, which can further identify the superconducting phases. Figure 3 shows the field-sweep resistivity at different temperatures under a perpendicular field (results for the in-plane field are in the Supplemental Material [17]) with different behavior for $\alpha$-BiPd, $\beta$-$Bi_2Pd$, and $\gamma$-BiPd. For $\gamma$-BiPd, the same narrow transition shifts to higher fields at lower temperatures. However, for $\alpha$-BiPd and $\beta$-$Bi_2Pd$, pronounced field-induced phase transitions are observed at lower temperatures. In particular, $\alpha$-BiPd shows multiple plateau behaviors suggesting multiple superconducting phases, as shown in Fig. 3(a). We show the superconducting phase diagrams of $\alpha$-BiPd for the out-of-plane field in Fig. 3(b) by identifying the onset of abrupt changes in the transition to determine $H_{c2}$. At 2.8 K, a multicritical point intersects with the strong kink in the $H_{c2}(T)$ curve, revealing the presence of three superconducting states. In the first region of the superconductive state (blue circle points) in Fig. 3(b), $H_{c2}$ follows the linear GL formula presented in Eq. (1), suggesting the spin-singlet state with even parity. In the third region (the red star points) in Fig. 3(b), $H_{c2}$ increases sharply at $T < 2.8$ K suggesting the spin-triplet state with odd parity. In between the spin-triplet and spin-singlet states lies the admixture of the singlet-triplet state (orange triangle points) in Fig. 3(b), where $H_{c2}$ exhibits

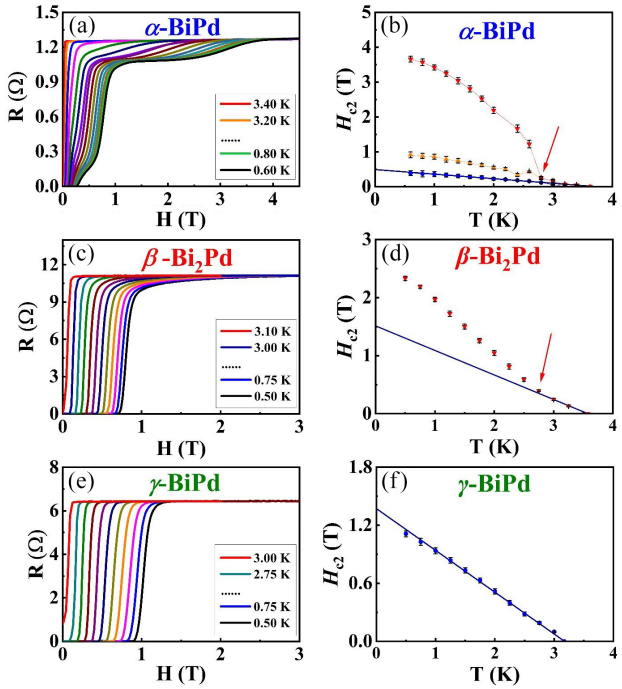


FIG. 3. The field-sweep resistivity at different temperatures under a perpendicular field for (a) $\alpha$-BiPd, (c) $\beta$-$Bi_2Pd$, and (e) $\gamma$-BiPd. The temperature dependence of the upper critical field in (b) $\alpha$-BiPd, (d) $\beta$-$Bi_2Pd$, and (f) $\gamma$-BiPd. The solid curves are the best fits to the GL relationships. The red arrows in (b) and (d) indicate the kink point.

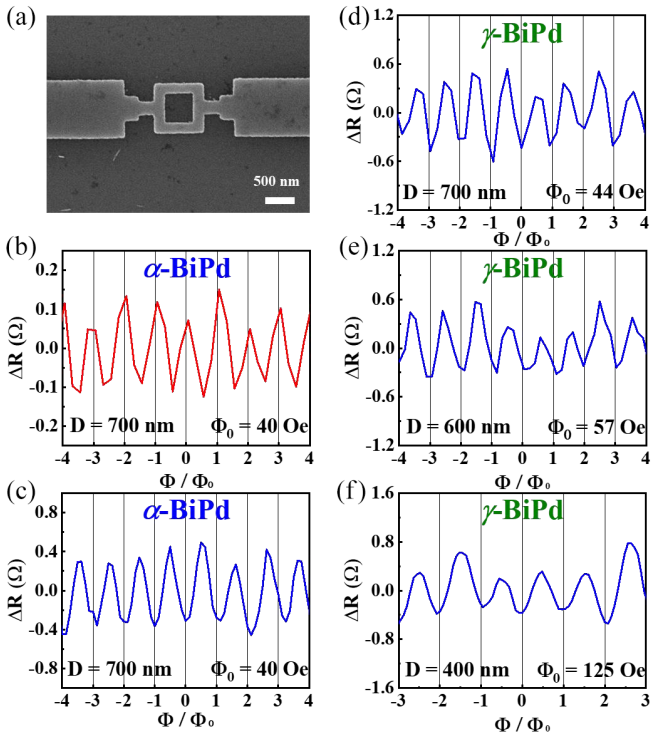


FIG. 4. (a) The scanning electron microscope image of a representative superconducting ring device. Little-Parks effect of $\alpha$-BiPd in the dimension of D = 700 nm with (b) half-integer and (c) integer flux quantization. Little-Parks effect of $\gamma$-BiPd devices with integer flux quantization in (d) $D = 700$, (e) $D = 600$, and (f) D = 400 nm.

unconventional behavior but with a smaller magnitude. Although $\alpha$-BiPd exhibits anomalous kink behaviors regardless of the external field direction, multiphase superconductivity can only be observed when the field is applied in the out-of-plane but not in the in-plane direction (as shown in the Supplemental Material [17]). The multiphase superconductivity in the out-of-plane field is due to the noncentrosymmetric nature of the $\alpha$-BiPd thin film, which has a broken inversion symmetry along the out-of-plane direction as shown by the pole-figure measurement (see Supplemental Material [17]).

In the case of $\beta$-$Bi_2Pd$, it exhibits only one kink transition, as shown in Figs. 3(c) and 3(d) at $T < 2.7$ K, consistent with its centrosymmetric triplet pairing. Finally, in centrosymmetric $\gamma$-BiPd, its $H_{c2}$ displays a narrow transition width across different temperatures, as shown in Fig. 3(e), with a linear temperature dependence [Fig. 3(f)]. The linear and the square root temperature dependence of $H_{c2}(\mathrm{T})$ for the out-of-plane magnetic field and for the in-plane magnetic field (as shown in Fig. S6 [17]) can both be described by the BCS GL theory, as expected for a spin-singlet SC.

We have also resorted to phase-sensitive flux quantization (Little-Parks effect) measurements in polycrystalline rings to assess pairing. The single-value nature of the complex macroscopic superconducting wave function necessitates a universal $2\pi$ phase shift in any closed path around a ring, resulting in magnetic flux quantization of $n\Phi_o$ [22]. In even-parity spin-singlet SCs (e.g., Nb), the superconducting gap does not change sign upon inversion at the grain boundaries, always leading to integer flux $n\Phi_o$ (0 rings). However, in odd-parity spin triplet SCs, a sign change in the gap value triggers a $\pi$ phase shift. A total even number of $\pi$ phase shifts gives integer flux $n\Phi_o$, whereas an odd number of $\pi$ phase shifts gives half-integer flux $(n + ½)\Phi_o$ ($\pi$ rings). There are equal integer and half-integer flux occurrences in spin-triplet rings but different proportions in an admixture of singlet-triplet rings. All of these different features have been observed in our rings of $\gamma$-BiPd, $\beta$-$Bi_2Pd$, and $\alpha$-BiPd.

As shown in Fig. 4(a), we fabricate our polycrystalline films into submicron-sized square ring devices by electron beam lithography and ion beam etching. Because $\Phi_0 \approx 20$ Oe$(\mu\mathrm{m})^2$, we design the dimensions of the rings with an area near $(1\ \mu\mathrm{m})^2$ so that the oscillation period of the magnetic field varies in the range of 20 to 150 Oe for accurate measurements. With the ring devices at a constant temperature near $T_C$, the magnetic field causes oscillations in free energy in increments of $\Phi_o$. In all cases, the measured values of $\Phi_o$ are consistent with ring areas from electron microscopy with an example shown in Fig. 4(a). In $\alpha$-BiPd, the observed oscillation period of 40 Oe agrees

TABLE I. Unequivocal identification of spin-singlet, spin-triplet, and singlet-triplet admixture in centrosymmetric and noncentrosymmetric SCs by upper critical field and flux quantization.

| Pairing | Spin singlet | Spin triplet | Singlet-triplet admixture |
|---|---|---|---|
| Crystal symmetry | Centrosymmetric | Centrosymmetric | Noncentrosymmetric |
| Superconductors | $\gamma$-BiPd | $\beta$-$Bi_2Pd$ | $\alpha$-BiPd |
| Upper critical field | BCS-like behavior | Kink behavior | Kink behavior |
| Flux quantization | | Integer (~50%) | Integer (>50%) |
| | Integer (100%) | Half-integer (~50%) | Half-integer (<50%) |

well with the expected values of 40.8 Oe and shows half-quantization with the resistance minima occurring at the half-integer of $\Phi = (n + 1/2)\Phi_0$, indicating $\pi$ rings with half quantum flux (HQF) resulting from the odd parity of spin-triplet pairing. We have performed various experiments to ascertain negligible trap flux (Supplemental Material [17]). In addition to $\pi$ rings, we have also observed 0 rings with integer flux $n\Phi_o$ in other $\alpha$-BiPd rings, where the resistance minima occur at the integer quantization, as shown in Fig. 4(c). On the other hand, in centrosymmetric $\gamma$-BiPd rings of different sizes (700, 600, and 400 nm) with expected periods of oscillation $\Phi_o = 40.8$, 55.6, and 125 Oe, respectively, we observed *only* 0 rings with integer flux quantization (0 ring), indicating pure singlet-pairing, as shown in Figs. 4(d)–4(f).

Experimentally, all 20 rings of $\gamma$-BiPd are 0 rings with no $\pi$ rings. In contrast, in the case of $a$-BiPd rings, 17 are 0 rings and only 3 are $\pi$ rings, indicating that approximately 15% of polycrystalline $\alpha$-BiPd devices are $\pi$ rings. This finding is consistent with a recent study of $\alpha$-BiPd that reported a 20% occurrence rate [23]. On the other hand, for polycrystalline rings of centrosymmetric $\beta$-$Bi_2Pd$ with a pure spin-triplet pairing state, there is an equal probability for a $\pi$ ring and 0 ring [10]. The proportion of the $\pi$ ring is 0 (singlet $\gamma$-BiPd) and 50% (triplet $\beta$-$Bi_2Pd$) of the centrosymmetric SCs and a value lower than 50% (admixture singlet-triplet $\alpha$-BiPd) for the noncentrosymmetric SCs depending on the degree of admixture. These are decisive assessments for centrosymmetric and noncentrosymmetric SCs.

In summary, as shown in Table I, we demonstrate that the kink-point upper critical field and the phase-sensitive flux quantization measurements can both unequivocally reveal centrosymmetric singlet ($\gamma$-BiPd), centrosymmetric triplet ($\beta$-$Bi_2Pd$) SCs, as well as the noncentrosymmetric singlet-triplet admixture ($\alpha$-BiPd). The unusual kink $H_{c2}$ behavior that exceeds the orbital pair-breaking limit indicates the existence of spin-triplet state pairing in $\alpha$-BiPd and $\beta$-$Bi_2Pd$. In the phase-sensitive measurement, the observation of the half-quantum flux reveals triplet pairing. These two methods are essential for identifying triplet superconductors and exploring their quantum properties, including Majorana physics and flux qubits for quantum computing.

The authors thank Yufan Li and Xiaoying Xu (Johns Hopkins University) for fruitful discussion; Yen-Chun Chen, Xiao-Cheng Lu, and Li-Zai Tsai (Academia Sinica) for E-beam lithography support; Yen-Chang Tu, Hsia-Ling Liang, and Tsao-Chi Chuang (National Taiwan University) for experimental support, and the Quantum Materials Shared Facilities of the Institute of Physics at Academia Sinica. We acknowledge support by the Ministry of Science and Technology of Taiwan under Grants No. MOST 110-2123-M-002-010 and No. MOST 110-2112-M-002-047-MY3, U.S. DOE Grant No. DE-SC0009390, Center of Atomic Initiative for New Materials (AI-MAT), National Taiwan University, within Higher Education Sprout Project by the Ministry of Education in Taiwan. C. C. Chiang was supported by the National Science and Technology Council of Taiwan via the Graduate Students Study Abroad Program under Grant No. 112-2917-I-002-001.

C. C. C., C. L. C., and S. Y. H. conceived the project. C. C. C. and H. C. L. characterized the thin film samples. C. C. C. and C. D. C. conducted the e-beam lithography. C. C. C. and H. C. L. conducted the electrical transport measurements. S. C. L. and M. W. C. conducted the x-ray pole figure measurement. C. C. C. drafted the original manuscript. D. Q., C. L. C., and S. Y. H. reviewed and revised the manuscript with contributions from all.

*Corresponding author: clchien@jhu.edu
†Corresponding author: syhuang@phys.ntu.edu.tw

[1] F. Arute, K. Arya, R. Babbush *et al.*, Nature (London) **574**, 505 (2019).
[2] J. Alicea, Rep. Prog. Phys. **75**, 076501 (2012).
[3] F. Wilczek, Nat. Phys. **5**, 614 (2009).
[4] M. Sato and Y. Ando, Rep. Prog. Phys. **80**, 076501 (2017).
[5] Y. Maeno, S. Kittaka, T. Nomura, S. Yonezawa, and K. Ishida, J. Phys. Soc. Jpn. **81**, 011009 (2012).
[6] A. Pustogow, Y. Luo, A. Chronister *et al.*, Nature (London) **574**, 72 (2019).
[7] K. Ishida, M. Manago, K. Kinjo, and Y. Maeno, J. Phys. Soc. Jpn. **89**, 034712 (2020).
[8] C. C. Tsuei, J. R. Kirtley, C. C. Chi, Lock See Yu-Jahnes, A. Gupta, T. Shaw, J. Z. Sun, and M. B. Ketchen, Phys. Rev. Lett. **73**, 593 (1994).

[9] J. R. Kirtley, C. C. Tsuei, J. Z. Sun, C. C. Chi, L. S. Yu-Jahnes, A. Gupta, M. Rupp, and M. B. Ketchen, Nature (London) **373**, 225 (1995).
[10] Y. Li, X. Xu, M. H. Lee, M. W. Chu, and C. L. Chien, Science **366**, 238 (2019).
[11] S. Ran, C. Eckberg, Q. P. Ding, Y. Furukawa, T. Metz, S. R. Saha, I. L. Liu, M. Zic, H. Kim, J. Paglione, and N. P. Butch, Science **365**, 684 (2019).
[12] S. Khim, J. F. Landaeta, J. Banda, N. Bannor, M. Brando, P. M. R. Brydon, D. Hafner, R. Küchler, R. Cardoso-Gil, U. Stockert, A. P. Mackenzie, D. F. Agterberg, C. Geibel, and E. Hassinger, Science **373**, 1012 (2021).
[13] Z. Sun, M. Enayat, A. Maldonado, C. Lithgow, E. Yelland, D. C. Peets, A. Yaresko, A. P. Schnyder, and P. Wahl, Nat. Commun. **6**, 6633 (2015).
[14] S. Thirupathaiah, Soumi Ghosh, Rajveer Jha, E. D. L. Rienks, Kapildeb Dolui, V. V. Ravi Kishore, B. Büchner, Tanmoy Das, V. P. S. Awana, D. D. Sarma, and J. Fink, Phys. Rev. Lett. **117**, 177001 (2016).
[15] M. Sakano, K. Okawa, M. Kanou, H. Sanjo, T. Okuda, T. Sasagawa, and K. Ishizaka, Nat. Commun. **6**, 8595 (2015).
[16] M. Heise, J. H. Chang, R. Schonemann, T. Herrmannsdorfer, J. Wosnitza, and M. Ruck, Chem. Mater. **26**, 5640 (2014).
[17] See Supplemental Material at http://link.aps.org/supplemental/10.1103/PhysRevLett.131.236003 for more details on x-ray analysis, upper critical field extraction, the WHH analysis, and the Little-Parks measurement, which includes Ref. [18].
[18] K. Maki, Phys. Rev. **148**, 362 (1966).
[19] M. Tinkham, *Introduction to Superconductivity*, 2nd ed. (Dover Publications, New York, 2004).
[20] N. R. Werthamer, E. Helfand, and P. C. Hohenberg, Phys. Rev. **147**, 295 (1966).
[21] E. Helfand and N. R. Werthamer, Phys. Rev. **147**, 288 (1966).
[22] W. A. Little and R. D. Parks, Phys. Rev. Lett. **9**, 9 (1962).
[23] X. Xu, Y. Li, and C. L. Chien, Phys. Rev. Lett. **124**, 167001 (2020).